The Fundamental Plane of Elliptical Galaxies: Clues from Self-consistent Hydrodynamical Simulations

J. Oñorbe[1], R. Dominguez-Tenreiro[1], H. Artal[1] & A. Serna[2]

[1] Universidad Autónoma de Madrid; [2] Universidad Miguel Hernández (Elche)

1. INTRODUCTION

Elliptical galaxies populate a plane in the 3-parameter space of the observed effective radius, R_e^{light}, the mean surface brightness within that radius, $<I^{light}>_e$, and the central line-of-sight (los) velocity dispersion, $_{los,0}$, known as the Fundamental Plane (FP, [5], [6], [9], [13]):

$$\log R_e^{light} = a \cdot \log{}_{los,o} + b \cdot \log \langle I \rangle_e + c \qquad (1)$$

The values of the FP coefficients for the SDSS sample are a 1.5, similar in the four SDSS bands, b −0.77, and c −8.7 with a small scatter [2]. The existence of the FP and its small scatter has the important implication that it provides us with a strong constraint when studying elliptical galaxy formation and evolution.

On the other hand, in a theoretical perspective, assuming that ellipticals are dynamically hot systems whose configuration in phase space are close to equilibrium, the virial theorem predicts:

$$M_{vir} = \frac{c_F \left(\frac{tot}{3}\right)^2 r^{tot}}{G} \qquad (2)$$

where Mvir is the virial mass, $_{3,h}^{tot}$, is the average 3-dimensional velocity dispersion of dark and baryonic matter inside virial radius and $r_{e,h}^{tot}$, radius enclosing halos of the virial mass. We can connect observational results (Eq. 1) with theoretical predictions (Eq. 2) assuming that

$$L = 2 \cdot I_e \cdot R_e^2 \qquad (4) \qquad\qquad c_M^{vir} = c_F\, c_V\, c_R \qquad (5)$$

Equation (4) relates luminosity with the mean surface brightness and effective radius. Equation (5) simply include the coefficients that relate characteristics parameters of observations with theoretical predictions:

$$c_v = \frac{\left(\frac{tot}{3}\right)^2}{3 \cdot \left(\frac{star}{los,0}\right)^2} \quad (6) \qquad\qquad c_r = \frac{r_{vir}}{R_e^{ob}} \quad (7)$$

2. THE PHYSICS OF THE TILT

Finally from Eq. (2) and using Eq (4) and Eq. (5) one gets a relation similar to Eq. (1), the Virial Plane:

$$R_e = \frac{3}{G \cdot 2} \cdot c_M^{vir} \cdot \left(\frac{M_{vir}}{L}\right)^{-1} \cdot {}_{los,o}^2 \cdot I_e^{-1} \qquad (8)$$

The observational results described above mean that the FP its tilted relative to the virial plane. The origin of this tilt must be in the dependence of the following coefficients with luminosity

$$\left(c_M^{vir}\right)^{-1} \cdot \frac{M_{vir}}{M^{star}} \cdot \frac{M_{ob}^{star}}{L} \propto L^{obs} \qquad (9)$$

- 2.1. Stellar content: metallicity, age, IMF
$$\frac{M_{ob}^{star}}{L} \propto L^{stellar} \qquad (10)$$

- 2.2. Mass content: variation in the amount of dark matter with bright matter
$$\frac{M_{vir}}{M_{ob}^{star}} \propto L^{vir} \qquad (11)$$

- 2.3. Homology breaking: relation between characteristic parameters. Global structure of galaxies
$$\left(c_M^{vir}\right)^{-1} \propto L^u \qquad (12)$$

We can split this coefficient in kinematical and structural ratios

$$c_r = c_{r,D} \cdot c_{r,P} = \frac{r_{vir}}{r_e^{ob}} \cdot \frac{r_e^{ob}}{R_e^{ob}} \propto L^r \qquad\qquad c_v = c_{v,D} \cdot c_{v,PC} = \frac{\left(\frac{tot}{3}\right)^2}{\left(\frac{star}{3,bo}\right)^2} \cdot \frac{\left(\frac{star}{3,bo}\right)^2}{3 \cdot \left(\frac{star}{los,0}\right)^2} \propto L^v$$

This work consist in a detailed study of the possible origins of the tilt

3. METHOD: SIMULATIONS

The code used in our simulations is DEVA [17]. Gravity is computed through an AP3M-like method and hydrodynamics through a SPH technique where particular attention has been paid to the implementation of conservation laws.

64^3 DM particles and 64^3 GAS particles in a periodic box of 10 Mpc side; $_g$ = 2,33 kpc gravitational softening

We work in the framework of turbulent sequential star formation scenario [7]. In DEVA, cold locally-collapsing gas, denser than a threshold density, $_{thres}$, is transformed into stars in a timescale given by empirical Kennicutt-Schmidt law [12], with an average star formation efficiency, c_*, at scales resolved by the code.

3.1. ELOS

10 simulations: SF-A type: $_{thres}$ = 6x10-25 gr cm-3, c_* = 0.3
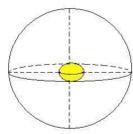SF-B type: $_{thres}$ = 1.8x10-24 gr cm-3, c_* = 0.1
Elliptical-like-objects (ELOs): identified as those objects having a dynamically relaxed stellar spherical component, with no disks and a very low gas content.

Samples:

EZ0-A ELO sample: 26 objects (black)
EZ0-B ELO sample: 17 objects (red)

4. RESULTS: THE SCALES

4.1. Halo scale: The virial theorem

Halo scale is parameterized by M_{vir}, dark and baryon mass enclosed in virial radius, $r_{e,h}^{tot}$, radius enclosed half the mass of these $_{tot}$ constituents within virial radii and $_{3,h}^{tot}$, average 3-dimensional velocity dispersion of dark and baryonic matter inside virial radius

We calculate C_F parameter (Eq. 2) for each ELO and calculate its dependence with the mass. See Fig. 1.
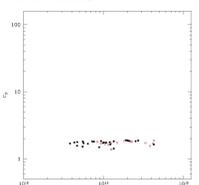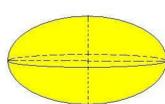
ELOs satisfy virial theorem at halo scale

Figure 1.

$$\frac{M_{vir}}{M_{ob}^{star}}$$

$$c_{r,D} = \frac{r_{e,h}^{tot}}{r_{e,ob}^{star}}$$

$$c_{v,D} = \frac{\left(\frac{tot}{3}\right)^2}{\left(\frac{star}{3,bo}\right)^2}$$

4.2. ELO scale: 3D galaxy

ELO scale is parameterized by M_{ob}^{star}, star mass of the baryonic object, $r_{e,ob}^{star}$, radii enclosed half the M_{ob}^{star} and $_{3,bo}^{star}$, mean square velocity for stars.

$$\frac{M_{ob}^{star}}{M_{cyl,ob}^{star}} \simeq 1$$

$$c_{r,P} = \frac{r_{e,ob}^{star}}{R_{e,ob}^{star}}$$

$$c_{v,PC} = \frac{\left(\frac{star}{3,bo}\right)^2}{3 \cdot \left(\frac{star}{los,0}\right)^2}$$

4.3. Projected ELO scale: What we see
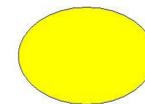
Projected ELO characteristic mass is parameterized by $M_{cyl,ob}^{star}$, star mass of the baryonic object. This mass is almost equal to the characteristic mass of ELO scale. The other characteristic Parameters are $R_{e,ob}^{star}$, radii enclosed half the $M_{cyl,ob}^{star}$ and $_{los,0}^{star}$, central stellar line-of-sight velocity dispersion.

To calculate characteristic parameters of this scale, we use three orthogonal projections. Firstly we use the mean for these three projections. To make more test we also build samples of ELOs with random projections (see below).

5. Halo scale to ELO scale: Physic of the baryons

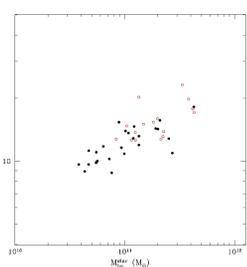### 5.1. Dark Matter vs.. Bright Matter content:

Fig. 4: Relation of virial mass and stellar mass for SF-A sample (black) and SF-B sample (red). The mass fraction of stars bound to the ELOs (or, more generically, cold baryons) relative to total mass within the virial radius, decrease with the mass scale

$$\frac{M_{vir}}{M_{ob}^{star}} \propto \left(M_{ob}^{star}\right)^{vir}$$

$$\beta_{vir,A} = 0.221 \pm 0.083$$

$$\beta_{vir,B} = 0.281 \pm 0.048$$

The dark to bright mass content of ELOs increases with their mass. See Conclusions.

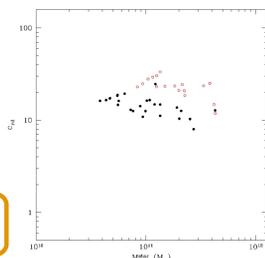### 5.2. Dark Matter vs.. Bright Matter distribution:

$$c_{r,D} \propto \left(M_{ob}^{star}\right)^{r,D}$$

$$\beta_{rD,A} = -0.225 \pm 0.127$$

$$\beta_{rD,B} = -0.316 \pm 0.199$$

Fig. 3: C_{rD} for SF-A sample (black) and SF-B sample (red)
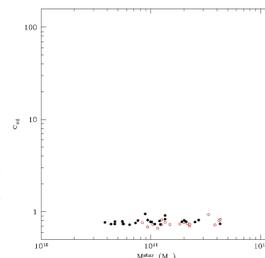
We find a clear trend with the mass. See Conclusions.

5.3. Dark Matter vs.. Bright matter kinematics

$$c_{v,D} \propto \left(M_{ob}^{star}\right)^{v,D}$$
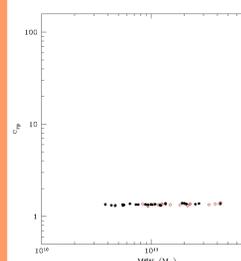
$$\beta_{vD,A} = 0.021 \pm 0.041$$

$$\beta_{vD,B} = 0.076 \pm 0.075$$

Fig. 4: C_{rD} for SF-A sample (black) and SF-B sample (red). No trend with mass is observed

6. ELO scale to Observational variables: Projection effects

6.1. 3D vs.. Projected bright matter distribution

Fig. 5: $C_{r,P}$ for SF-A sample (black) and SF-B sample (red). We can see the good correlation between 3D ELO scale radius and "observational" projected ELO scale radius. No trend with mass is observed.
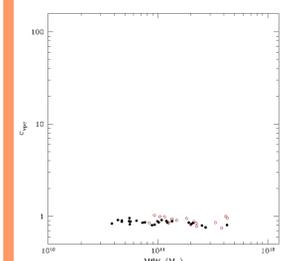
$$c_{r,P} \propto \left(M_{ob}^{star}\right)^{r,P}$$

$$\beta_{rP,A} = 0.019 \pm 0.009$$

$$\beta_{rP,B} = 0.016 \pm 0.017$$

6.2. 3D vs. Projected bright matter Kinematics

Fig. 6: $C_{v,PC}$ for SF-A sample (black) and SF-B sample (red). We can see the good correlation between 3D ELO scale velocity dispersion and "observational" line-of-sight velocity dispersion ELO. No trend with mass is observed.

$$c_{v,PC} \propto \left(M_{ob}^{star}\right)^{v,PC}$$

$$\beta_{vPC,A} = -0.044 \pm 0.029$$

$$\beta_{vPC,B} = -0.044 \pm 0.093$$

6.3. Influence on the scatter of the Fundamental Plane

Although projection effects seems not to play a important role in the origin of the tilt, we have study its effect by building random ELO samples choosing one projection for each ELO. We have found the same trends for C_{rP} and C_{vPC} but for an increase of the scatter.

7. CONCLUSIONS

- We find ELOs satisfy virial theorem at halo scale
- We find systematic trends with mass scale in:
  - Dark matter vs. Bright matter content: The mass fraction of stars decrease with the mass scale
  - Dark matter vs. Bright matter distribution: Homology breaking
- These trend do not significantly depend on the star formation parameterization.
- Both are due to systematic decrease, with increasing ELO mass, of the relative amount of dissipation experienced by the baryonic mass component along ELO formation [1][10][4].
- These trends cause a tilt of the virial plane in such a way that there is no further need of any relevant contribution from stellar population effects to explain observed tilt.
- Projection effects do not play an important role in the origin of the tilt of the FP but they increase the scatter.

7.1. Summary of fits

- Matter content:

	β_{vir}
SF-A	0.221± 0.083
SF-B	0.237 ± 0.158

- Homology breaking:

	β_{rD}	β_{vD}	β_{rP}	β_{vPC}
SF-A	-0.225 ± 0.127	0.021 ± 0.041	0.019 ± 0.009	-0.044 ± 0.029
SF-B	-0.316 ± 0.199	0.076 ± 0.075	0.016 ± 0.017	-0.044 ± 0.093

All $_i$ slopes are obtained through direct fits. Errors are 95% confidence intervals.

8. REFERENCES

[1] Bender, R., Burstein, D., & Faber, S.M. 1992 ApJ, 399, 462
[2] Bernardi, M., et al. 2003 AJ, 125,1866
[3] Ciotti, L., Lanzoni, B. & Renzini, A. 1996, MNRAS, 282,1
[4] Djorgovski, S. & Davis, M. 1987, ApJ, 389, L49
[5] Dressler, G. et al. 1987, ApJ, 313, 42
[6] Elmegreen & Scale astroph/0404451 preprint
[7] Faber, S.F. et al. 1987, in Nearly Normal Galaxies: From the Planck Time to the Present, ed. S.M. Faber (New York: Springer), 175
[8] Guzmán, R. et al. 1993, MNRAS, 265, 731
[9] Kennicut, R. 1998, ApJ, 498,541
[10] Kormendy, J. & Djorgovski, S. 1989, ARA&A, 27, 235
[11] Serna, A. Domínguez-Tenreiro, R. & Sáiz, A., 2003, ApJ, 597, 878

Any comments or suggestions are very welcome: jose.onnorbe@uam.es Thank you!